Solar Phys (2015) 290:1323–1335
DOI 10.1007/s11207-015-0682-3

Non-reflective Propagation of Kink Pulses in Magnetic Waveguides in the Solar Atmosphere

N.S. Petrukhin[1] · M.S. Ruderman[2,3] · E. Pelinovsky[4,5]

Received: 24 January 2015 / Accepted: 6 April 2015 / Published online: 15 April 2015

Abstract We study the propagation of pulses of kink waves in magnetic-flux tubes. We use the thin-tube approximation and assume that the dependence of the phase speed on the distance along the tube is either linear or quadratic. In this case, the wave equation describing the propagation of kink waves reduces to the Klein–Gordon equation with constant coefficients. We present the general solution of the initial value–boundary value problem for this equation. Using this solution, we study the general properties of non-reflective pulse propagation. Then we apply the general results to the kink-pulse propagation in coronal magnetic loops. In particular, we suggest an alternative mechanism of small-amplitude decay-less kink oscillations in coronal loops.

Keywords Corona · Coronal magnetic loops · Waves · Wave reflection

1. Introduction

Propagating kink waves have been observed in spicules (Zaqarashvili *et al.*, 2007), in mottles (Kuridze *et al.*, 2012), in active-region fibrils (Pietarila *et al.*, 2011), in filament threads (Lin *et al.*, 2007; Okamoto *et al.*, 2007), and in coronal loops (Tomczyk *et al.*, 2007; Tian *et al.*, 2012). Common to all of these phenomena is the transverse displacement of a magnetic tube that is caused by an external driver. Then the perturbation caused by this displacement propagates along the tube. It is usually detected as a temporal variation of the magnetic-tube

✉ M.S. Ruderman
m.s.ruderman@sheffield.ac.uk

1 Higher School of Economics, National Research University, Moscow, Russia

2 Solar Physics and Space Plasma Research Centre (SP2RC), School of Mathematics and Statistics, University of Sheffield, Hicks Building, Hounsfield Road, Sheffield, S3 7RH, UK

3 Space Research Institute (IKI), Russian Academy of Sciences, Moscow, Russia

4 Department of Nonlinear Geophysical Processes, Institute of Applied Physics, Nizhny Novgorod, Russia

5 Nizhny Novgorod State Technical University n.a. R.E. Alekseev, Nizhny Novgorod, Russia

position. The propagating waves can be excited by a periodic driver acting at a fixed position on the magnetic tube. This mechanism was considered by Verth, Terradas, and Goossens (2010) and Terradas, Goossens, and Verth (2010) to explain the observed waves propagating along the coronal magnetic field reported by Tomczyk *et al.* (2007) and Tomczyk and McIntosh (2009). The periodic driving generates periodic waves that propagate along a magnetic tube.

Another mechanism that generates transverse waves in magnetic tubes is an impulsive transverse displacement of the tube. It generates a perturbation of the magnetic tube that is a superposition of fast-kink eigenmodes, each with its own amplitude. In the absence of dispersion, the initial wave form would keep its original shape during its propagation. Recently, the propagation of impulsively excited fast-kink waves along a homogeneous magnetic tube was studied by Oliver, Ruderman, and Terradas (2014).

Real magnetic-flux tubes in the solar atmosphere are inhomogeneous, with the density varying along and across the tube, and the tube cross-section radius varying along the tube. The density variation across the tube can cause wave damping due to resonant absorption. In this article we do not consider this phenomenon and concentrate on the effect of density and tube cross-section radius variation along the tube. In general, this variation causes wave reflection. Hence, even when a driver is situated at the tube footpoint and generates waves propagating from this footpoint along the tube, at some distance from the footpoint waves propagating in the opposite direction are also present. However, it is often observed that the reflected waves are practically absent and the waves generated by a driver only propagate in one direction. In particular, this is the case for propagating kink waves in coronal loops. They propagate from the footpoint to the loop apex (Tomczyk *et al.*, 2007). To explain this phenomenon, Ruderman *et al.* (2013) (Article 1 in what follows) suggested that the density and cross-section radius vary along the loop in a way corresponding to the non-reflective propagation of kink waves. They then studied the non-reflective propagation of periodic kink waves. Note that in application to solar physics, the non-reflective wave propagation has also been studied by Petrukhin, Pelinovsky, and Batsyna (2012).

In this article we aim to study non-reflective propagation of kink-wave pulses in magnetic tubes. This study can be considered as the generalisation of two studies: one presented in Article 1, and the other by Oliver, Ruderman, and Terradas (2014). However, the analysis in this article is much simpler than that of Oliver, Ruderman, and Terradas (2014) because we use the thin-tube approximation, while Oliver, Ruderman, and Terradas carried out the analysis without any assumptions about the ratio of the tube radius to the characteristic perturbation length. This article is organised as follows: In the next section we formulate the problem and write down the governing equations. In Section 3 we briefly describe the reduction of the wave equation to the Klein–Gordon equation and formulate the conditions where it describes the non-reflective wave propagation. In Section 4 we present the solution of the initial value–boundary value problem. In Section 5 we investigate the general properties of pulse propagation in non-reflective wave guides. In Section 6 we apply the general results to kink-pulse propagation in coronal loops. Section 7 contains the summary of the results and our conclusions.

2. Problem Formulation

We consider kink-wave propagation along a straight magnetic tube in the cold-plasma approximation. We assume that the tube cross-section is circular, and its radius can vary along the tube. The plasma density can also vary along the tube, but does not vary across the tube.

Hence, in cylindrical coordinated $[r, \varphi, z]$ with the z-axis coinciding with the tube axis, the plasma density is given by

$$\rho = \begin{cases} \rho_{\mathrm{i}}(z), & r < R(z), \\ \rho_{\mathrm{e}}(z), & r > R(z), \end{cases} \tag{1}$$

where $R(z)$ is the radius of the tube cross-section. In the thin-tube approximation, plane-polarised kink waves are described (Ruderman, Verth, and Erdélyi, 2008) by

$$\frac{\partial^2(\eta/R)}{\partial t^2} - c_{\mathrm{k}}^2(z)\frac{\partial^2(\eta/R)}{\partial z^2} = 0, \tag{2}$$

where η is the tube displacement, c_{k} the kink speed, defined by

$$c_{\mathrm{k}}^2(z) = \frac{B^2(z)}{\mu_0[\rho_{\mathrm{i}}(z) + \rho_{\mathrm{e}}(z)]}, \tag{3}$$

μ_0 the magnetic permeability of free space, and B the magnetic-field magnitude related to the tube radius by

$$B(z)R^2(z) = \text{const.} \tag{4}$$

Equation (2) is used below to study non-reflective propagation of kink-wave pulses.

3. General Theory

A solution to Equation (2) in the form

$$u(z,t) \equiv \eta(z,t)/R(z) = A(z)\Phi\big(\tau(z), t\big), \tag{5}$$

with

$$\tau(z) = \int \frac{\mathrm{d}z}{c_{\mathrm{k}}(z)}, \qquad A(z) = c_{\mathrm{k}}^{1/2}(z), \tag{6}$$

reduces Equation (2) to the variable-coefficient Klein–Gordon equation (see Article 1)

$$\frac{\partial^2\Phi}{\partial t^2} - \frac{\partial^2\Phi}{\partial \tau^2} = \frac{c_{\mathrm{k}}^2}{A}\frac{\mathrm{d}^2A}{\mathrm{d}z^2}\Phi. \tag{7}$$

This equation reduces to the Klein–Gordon equation with constant coefficients,

$$\frac{\partial^2\Phi}{\partial t^2} - \frac{\partial^2\Phi}{\partial \tau^2} = \beta\Phi, \tag{8}$$

where β is a constant, when $c_{\mathrm{k}}(z)$ is either linear or quadratic function of z, *i.e.* when either

$$c_{\mathrm{k}} = \pm 2\sqrt{|\beta|}(z + L), \quad \beta < 0, \tag{9}$$

or

$$c_{\mathrm{k}} = M(z + N)^2 + \frac{\beta}{M}, \tag{10}$$

where M and N are constant. In what follows, we assume that perturbations are generated at $z = 0$. If we assume that they propagate in the positive z-direction along an unbounded magnetic tube, then $z \in [0, \infty)$. To have $c_k(z)$ positive, we have to choose the $+$ sign in Equation (9) and take $L > 0$. Similarly, we have to impose the conditions that either

$$\beta > 0, \qquad M > 0, \tag{11}$$

or

$$\beta < 0, \qquad M > 0, \qquad N > 0, \qquad M^2 N^2 > |\beta|. \tag{12}$$

However, propagating kink waves are also observed in coronal magnetic loops (Tomczyk *et al.*, 2007; Tian *et al.*, 2012), which are wave guides of finite length. They are driven at one loop footpoint. There is no reflection from the other footpoint because the waves damp before they reach it. A suitable form of $c_k(z)$ for coronal loops is one given by Equation (10) with

$$M < 0, \qquad N = -\ell, \qquad \beta < -M^2 \ell^2, \tag{13}$$

where ℓ is the loop half-length.

When $c_k(z)$ is defined by Equation (9) with the $+$ sign, the function $\tau(z)$ is given by

$$\tau(z) = \frac{\ln(z/L + 1)}{2\sqrt{|\beta|}}, \tag{14}$$

where we have imposed the condition $\tau(0) = 0$. When $c_k(z)$ is defined by Equation (10), the function $\tau(z)$ is given by

$$\tau(z) = \frac{1}{\sqrt{\beta}} \left(\arctan \frac{M(z+N)}{\sqrt{\beta}} - \arctan \frac{MN}{\sqrt{\beta}} \right) \tag{15}$$

when $\beta > 0$, and by

$$\tau(z) = \frac{1}{2\sqrt{|\beta|}} \ln \frac{[M(z+N) - \sqrt{|\beta|}](MN + \sqrt{|\beta|})}{[M(z+N) + \sqrt{|\beta|}](MN - \sqrt{|\beta|})} \tag{16}$$

when $\beta < 0$ and $M > 0$. Finally,

$$\tau(z) = \frac{1}{2\sqrt{|\beta|}} \ln \frac{[\sqrt{|\beta|} + |M|(z-\ell)](\sqrt{|\beta|} + \ell|M|)}{[\sqrt{|\beta|} - |M|(z-\ell)](\sqrt{|\beta|} - \ell|M|)} \tag{17}$$

when $\beta < 0$ and $M < 0$. When deriving Equations (15)–(17), we again imposed the condition $\tau(0) = 0$.

When the dependence of the phase speed on z is linear, it follows from Equation (14) that $\tau \to \infty$ as $z \to \infty$, so in this case Equation (8) has to be solved for $\tau \in [0, \infty)$. On the other hand, when the dependence of the phase speed on z is quadratic, it follows from Equations (15) and (16) that $\tau \to \tau_0$ as $z \to \infty$, where

$$\tau_0 = \begin{cases} \frac{1}{\sqrt{\beta}} \left(\frac{\pi}{2} - \arctan \frac{MN}{\sqrt{\beta}} \right), & \beta > 0 \\ \frac{1}{2\sqrt{|\beta|}} \ln \frac{MN + \sqrt{|\beta|}}{MN - \sqrt{|\beta|}}, & \beta < 0. \end{cases} \tag{18}$$

Hence, in the case of a quadratic phase-speed profile given by Equation (10) with $M > 0$, we solve Equation (8) for $\tau \in [0, \tau_0)$. Finally when the phase speed is given by Equation (10)

with $M < 0$, we solve Equation (2) for $z < 2\ell$. This implies that we solve Equation (8) for $\tau \in [0, \tau_1)$, where

$$\tau_1 = \tau(2\ell) = \frac{1}{\sqrt{|\beta|}} \ln \frac{\sqrt{|\beta|} + \ell|M|}{\sqrt{|\beta|} - \ell|M|}. \tag{19}$$

4. General Solutions Describing Pulse Propagation

We assume that the magnetic-flux tube is perturbed at its footpoint, *i.e.* at $z = 0$, and it is at rest at the initial moment of time. Hence, we impose the initial conditions

$$u = \frac{\partial u}{\partial t} = 0 \quad \text{at } t = 0,\ z \geq 0. \tag{20}$$

In addition, we impose the boundary condition

$$u = u_0(t) \quad \text{at } z = 0,\ t \geq 0. \tag{21}$$

In what follows we assume that the perturbation has the form of a pulse, *i.e.* $u_0(t) \to 0$ as $t \to \infty$. In addition, to have consistency between the initial and boundary conditions, we assume that $u_0(0) = u_0'(0) = 0$. Using Equations (5) and (6), we transform the boundary condition in Equation (21) to

$$\Phi = c_{\mathrm{k}}^{-1/2}(0) u_0(t) \equiv \Phi_0(t) \quad \text{at } \tau = 0,\ t \geq 0. \tag{22}$$

The initial conditions (20) are reduced to

$$\Phi = \frac{\partial \Phi}{\partial t} = 0 \quad \text{at } t = 0,\ \tau \geq 0. \tag{23}$$

The consistency condition between the initial and boundary conditions reduces to $\Phi_0(0) = \Phi_0'(0) = 0$.

When $c_{\mathrm{k}}(z)$ is a linear function, $\tau \in [0, \infty)$ and we impose the additional boundary condition $\Phi \to 0$ as $\tau \to \infty$. In the case when $c_{\mathrm{k}}(z)$ is a quadratic function with $M > 0$, $\tau \in [0, \tau_0)$ and the perturbation reaches infinity at finite time, which is, of course, unphysical. In this case, we therefore only consider the perturbation propagation for a time shorter than that necessary for the perturbation to reach infinity. Hence, in this case we also formally impose the condition $\Phi \to 0$ as $\tau \to \infty$. To justify this condition, we can, for example, assume that $c_{\mathrm{k}}(z)$ is a quadratic function only for $z < z_*$, while it is linear for $z > z_*$, where z_* is sufficiently large, and impose the conditions that $c_{\mathrm{k}}(z)$ and $c_{\mathrm{k}}'(z)$ are continuous at $z = z_*$. Finally, in the case when $c_{\mathrm{k}}(z)$ is a quadratic function with $M < 0$, $\tau \in [0, \tau_1)$ and the perturbation reaches the other footpoint of the loop at finite time. In this case we only consider the perturbation propagation for a time shorter than that necessary for the perturbation to reach the other footpoint. Again we formally impose the condition $\Phi \to 0$ as $\tau \to \infty$. To justify this condition, we can extend $c_{\mathrm{k}}(z)$ as a smooth function beyond $z = \ell$. For this we first extend it using the quadratic profile with $M > 0$ to get $c_{\mathrm{k}}'(z) > 0$, and then further extend it as a linear function.

When $\beta = a^2 > 0$, the solution to Equation (8) with the initial conditions in Equation (23) and the boundary condition in Equation (22) is given by Budak, Samarski, and Tikhonov

(1964). It reads

$$\Phi(\tau,t)=\Phi_0(t-\tau)+a\tau\int_0^{t-\tau}\frac{I_1(a\sqrt{(t-\xi)^2-\tau^2})}{\sqrt{(t-\xi)^2-\tau^2}}\Phi_0(\xi)\,\mathrm{d}\xi, \tag{24}$$

where I_1 is the modified Bessel function of the first kind and of order one. Equation (24) is valid for $\tau\le t$, while $\Phi(\tau,t)=0$ when $\tau>t$.

When $\beta=-a^2<0$, the solution to Equation (8) with the initial conditions in Equation (23) and the boundary condition in Equation (22) is obtained in the Appendix. It reads

$$\Phi(\tau,t)=\Phi_0(t-\tau)-a\tau\int_0^{t-\tau}\frac{J_1(a\sqrt{(t-\xi)^2-\tau^2})}{\sqrt{(t-\xi)^2-\tau^2}}\Phi_0(\xi)\,\mathrm{d}\xi, \tag{25}$$

where J_1 is the Bessel function of the first kind and of order one. Again Equation (25) is valid for $\tau\le t$, while $\Phi(\tau,t)=0$ when $\tau>t$. It is interesting to note that Equation (24) can be obtained from Equations (25) by substituting $\mathrm{i}a$ for a.

When $c_k(z)$ is a quadratic function with $M>0$, we only consider the perturbation propagation for a time shorter than that needed for the perturbation to reach infinity, we impose the restriction $t<\tau_0$. In the case when $c_k(z)$ is a quadratic function with $M<0$, we only consider the perturbation propagation for a time shorter than that needed for the perturbation to reach the other loop footpoint. Hence, in that case we impose the restriction $t<\tau_1$.

5. General Properties of Propagating Pulses

In this section we study the general properties of pulse propagation. We start by considering very short pulses and take $\Phi_0(t)$ to be a non-negative function different from zero in the interval $(0,T)$ and equal to zero when $t\notin(0,T)$, and such that $\Phi_0'(0)=0$. We assume that $aT\ll 1$. In this case we can neglect the variation of the first multiplier in the integrands in Equations (24) and (25) and use the approximate expressions valid for $t>\tau+T$,

$$\Phi(\tau,t)\approx\Phi_0(t-\tau)+a\tau Q\frac{I_1(a\sqrt{t^2-\tau^2})}{\sqrt{t^2-\tau^2}},\quad \beta=a^2, \tag{26}$$

$$\Phi(\tau,t)\approx\Phi_0(t-\tau)-a\tau Q\frac{J_1(a\sqrt{t^2-\tau^2})}{\sqrt{t^2-\tau^2}},\quad \beta=-a^2, \tag{27}$$

where $Q=\int_0^T\Phi_0(t)\,\mathrm{d}t$. It is interesting to study the evolution of perturbation at fixed z or, which is the same, at fixed τ. For $t<\tau$ the plasma is at rest at this spatial position. Since $aT\ll 1$, the first term on the right-hand side of Equations (24) and (25) strongly dominates the second term for moderate values of τ when $\tau<t<\tau+T$. For $t>\tau+T$ the first term is zero and the perturbation evolution is defined by the second term. At this point the perturbation evolution in the case with $\beta>0$ is qualitatively different from that in the case with $\beta<0$.

We start the study of the perturbation behaviour for $t>\tau+T$ from the second case where $\beta<0$. It is instructive to write down the dispersion equation. If we take $\Phi\propto\exp(\mathrm{i}k\tau-\mathrm{i}\omega t)$ in Equation (8), then we obtain $\omega^2=k^2+a^2$, which implies that there is a cut-off frequency equal to a. Only harmonic perturbations with frequencies higher than a can propagate, while perturbations with lower frequencies are evanescent. Recalling the properties of $J_1(z)$, we

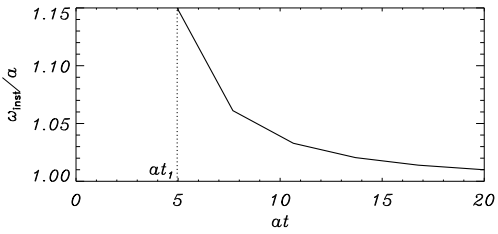

Figure 1 Dependence of instantaneous oscillation frequency $[\omega_{\text{inst}}]$ on time for $a\tau = \pi$.

see that the perturbation behaviour is oscillatory. Let j_n be the nth positive zero of $J_1(z)$, $n = 1, 2, \ldots$ Then $\Phi(\tau, t_n) = 0$, where $t_n = \sqrt{\tau^2 + a^{-2} j_n^2}$. We introduce the definition that the instantaneous period of oscillations at time t_n is equal to $2(t_{n+1} - t_n)$, and the oscillation frequency is $\omega_{\text{inst}} = \pi/(t_{n+1} - t_n)$. The instantaneous frequency $[\omega_{\text{inst}}]$ at time t such that $t_n < t < t_{n+1}$ is a linear function in the interval $[t_n, t_{n+1}]$, so that $\omega_{\text{inst}}(t)$ is a piecewise-linear function. The dependence of ω_{inst} on time is shown in Figure 1. We see that the instantaneous oscillation frequency decreases with time and only slightly deviates from the cut-off frequency a when $t \geq t_1$. Using the asymptotic formula (Abramowitz and Stegun, 1964)

$$J_1(z) \approx \sqrt{\frac{2}{\pi z}} \cos\left(z - \frac{3\pi}{4}\right), \quad z \gg 1, \tag{28}$$

we obtain that

$$\Phi(\tau, t) \approx a\tau Q \sqrt{\frac{2}{\pi a t^3}} \cos\left(at + \frac{\pi}{4}\right), \quad t \gg \max\left(a^{-1}, \tau\right). \tag{29}$$

Hence, for a long time, there are oscillations with the cut-off frequency at a fixed spatial position decaying as $t^{-3/2}$. Note that a similar behaviour was previously found by Rae and Roberts (1982) when studying the propagation of slow-sausage-wave pulses in thin magnetic-flux tubes.

In the case where $\beta > 0$ the perturbation behaviour is qualitatively different. In this case the dispersion equation is $\omega^2 = k^2 - a^2$, so there is no cut-off frequency. Using expansion of $I_1(z)$ in the power series, it is straightforward to show that the second term in Equation (26) is a monotonically increasing function of t. Hence, for $t > \tau + T$, the perturbation amplitude grows monotonically with time. We recall that we can only have $\beta > 0$ for a parabolic kink-velocity profile with $M > 0$. In this case we have imposed the restriction $t < \tau_0$. When $t \to \tau_0$ the perturbation amplitude tends to

$$A_{\max}(\tau) = a\tau Q \frac{I_1(a\sqrt{\tau_0^2 - \tau^2})}{\sqrt{\tau_0^2 - \tau^2}}. \tag{30}$$

It follows from Equation (18) that $\tau_0 < \pi/a$. Then it is straightforward to obtain that

$$A_{\max}(\tau) < A_{\text{lim}}(\tau) = \frac{a^2 \tau Q I_1(\sqrt{\pi^2 - a^2\tau^2})}{\sqrt{\pi^2 - a^2\tau^2}}. \tag{31}$$

A numerical investigation shows that the maximum value of the function

$$\frac{x I_1(\sqrt{\pi^2 - x^2})}{\sqrt{\pi^2 - x^2}}$$

is approximately equal to 1.95. Hence, we have $A_{\max}(\tau) < A_{\lim}(\tau) < 2aQ$. Since $Q = T\langle\Phi_0(t)\rangle$, where $\langle\Phi_0(t)\rangle$ is the mean value of function $\Phi_0(t)$ in the interval $[0, T]$, and $aT \ll 1$, we see that, for $T < t < \tau_0$, the perturbation amplitude remains much smaller than the amplitude of the initial pulse.

We also studied numerically the propagation of a pulse with longer duration. To do this, we introduced the dimensionless variables $\tilde{t} = at$ and $\tilde{\tau} = a\tau$ and rewrote Equations (24) and (25) in the dimensionless form as

$$\Phi(\tilde{\tau}, \tilde{t}) = \Phi_0(\tilde{t} - \tilde{\tau}) + \tilde{\tau} \int_0^{\tilde{t}-\tilde{\tau}} \frac{I_1(\sqrt{(\tilde{t} - \xi)^2 - \tilde{\tau}^2})}{\sqrt{(\tilde{t} - \xi)^2 - \tilde{\tau}^2}} \Phi_0(\xi)\, \mathrm{d}\xi \tag{32}$$

and

$$\Phi(\tilde{\tau}, \tilde{t}) = \Phi_0(\tilde{t} - \tilde{\tau}) - \tilde{\tau} \int_0^{\tilde{t}-\tilde{\tau}} \frac{J_1(\sqrt{(\tilde{t} - \xi)^2 - \tilde{\tau}^2})}{\sqrt{(\tilde{t} - \xi)^2 - \tilde{\tau}^2}} \Phi_0(\xi)\, \mathrm{d}\xi. \tag{33}$$

The boundary condition at $\tilde{\tau} = 0$ is given by

$$\Phi_0(\tilde{t}) = (\tilde{t}/\zeta)^2 \exp\left[1 - (\tilde{t}/\zeta)^2\right], \tag{34}$$

where $\zeta/a = T$ is the characteristic time of pulse duration at $\tau = 0$.

As we have pointed out, the perturbation evolution in the case where $\beta > 0$ is qualitatively different from that in the case where $\beta < 0$. When $\beta > 0$, Equation (8) is similar to the wave equation describing the density waves in a homogeneous self-gravitating medium (*e.g.* Zeldovich and Novikov, 1975). This equation admits solutions that unboundedly grow with time. These solutions describe the Jeans instability. The dispersion relations for Equation (8) and for the equation describing the density waves are the same. They read $\omega^2 = k^2 - a^2$. Hence, where $\beta > 0$, the solutions are unstable. This instability is not unphysical because for a non-reflective kink-speed profile that corresponds to $\beta > 0$, the wave escapes to infinity at a finite time.

The perturbation evolution at fixed τ is only shown for $\beta < 0$ because this case is more interesting from the point of view of applications than the case $\beta > 0$. Figures 2, 3, and 4 correspond to $\zeta = 0.5$, $\zeta = 1$, and $\zeta = 2$.

It is interesting to compare the results obtained in this section with those obtained by Cally (2012). Although Cally considered the Alfvén-wave propagation, the equation that he studied is the wave equation with variable phase speed, *i.e.* it coincides with Equation (2). Hence, from the mathematical point of view, the problem that we studied here and that studied by Cally are the same. In particular, Cally studied the Alfvén wave propagation in an atmosphere where the phase speed is proportional to $z^{(n-1)/(n-2)}$, where $n > 0$ and $n \neq 2$. When $n = 3$, we obtain that the phase speed is proportional to z^2, which is a particular case of the phase-speed profile given by Equation (2) corresponding to $\beta = 0$. Cally showed that there is no oscillatory wake after the main pulse when n is an odd integer. In particular, there is no wake when $n = 3$, *i.e.* when the phase speed is proportional to z^2. Obviously, this result does not contradict the results obtained in the present article. To obtain $c_k \propto z^2$, we need to take $\beta = 0$. In this case the Klein–Gordon equation (8) reduces to the wave equation with constant coefficients, which allows the d'Alembert solution. Hence, there is no wake in this case. As we showed above, an oscillatory wave only appears when $\beta < 0$.

6. Application to Kink Oscillations of Coronal Loops

The magnetic tubes with the best-known properties probably are coronal loops. Since, in addition, they are almost always thin with a cross-section radius much smaller than the

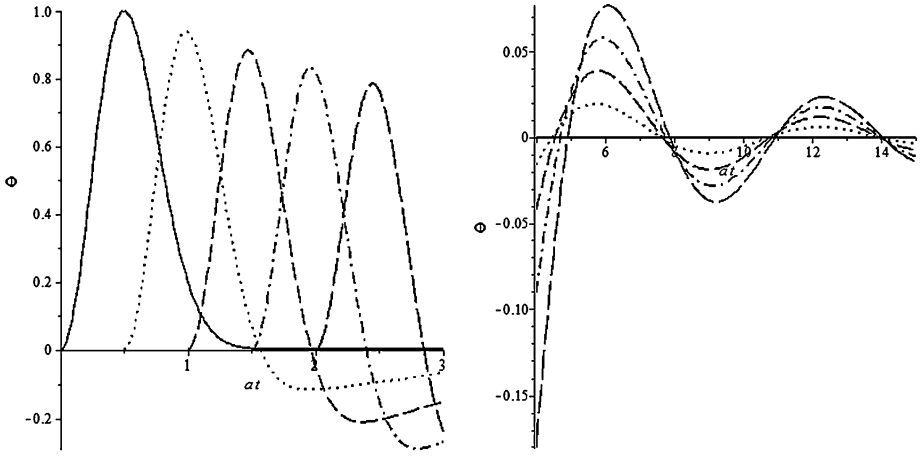

Figure 2 Dependence of the function Φ defined by Equation (33) on $\tilde{t} = at$ at fixed $\tilde{\tau} = a\tau$ for $\zeta = 0.5$. The solid, dotted, dashed, dashed–dotted, and long-dashed curves correspond to $\tilde{\tau} = 0$, 0.5, 1, 1.5, and 2. The left panel shows the dependence of Φ on $\tilde{t}$ for $\tilde{t} \leq 3$, while the right panel shows this dependence for $\tilde{t} \leq 14.5$. There is no solid curve in the right panel because $\Phi \approx 0$ at $\tilde{\tau} = 0$ for $\tilde{t} > 3$.

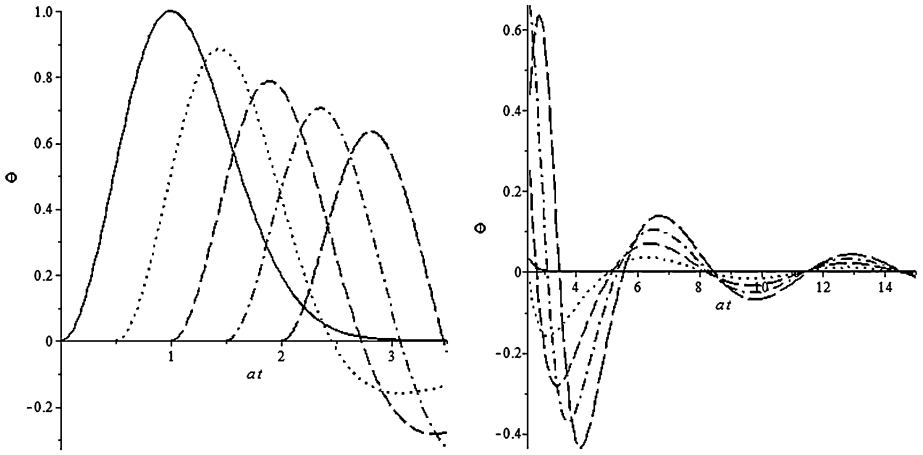

Figure 3 Dependence of the function Φ defined by Equation (33) on $\tilde{t} = at$ at fixed $\tilde{\tau} = a\tau$ for $\zeta = 1$. The solid, dotted, dashed, dashed–dotted, and long-dashed curves correspond to $\tilde{\tau} = 0$, 0.5, 1, 1.5, and 2. The left panel shows the dependence of Φ on $\tilde{t}$ for $\tilde{t} \leq 3.5$, while the right panel shows this dependence for $\tilde{t} \leq 14.5$. There is no solid curve in the right panel because $\Phi \approx 0$ at $\tilde{\tau} = 0$ for $\tilde{t} > 3.5$.

length, they are the best candidates for applying the theory developed in this article. Real coronal loops are characterised by a great variety of parameters. The plasma temperature inside the loop often differs from that outside, and the temperature varies along the loop. In addition, the loop shape differs from loop to loop. We do not aim to apply theoretical results to real observations. We only wish to present an example showing the qualitative properties of propagating pulses. We therefore use below the model of a coronal loop, which is the most popular in theoretical studies. It is a symmetric loop immersed in an isothermal atmosphere with the same plasma temperature inside and outside the loop. Since the kink speed

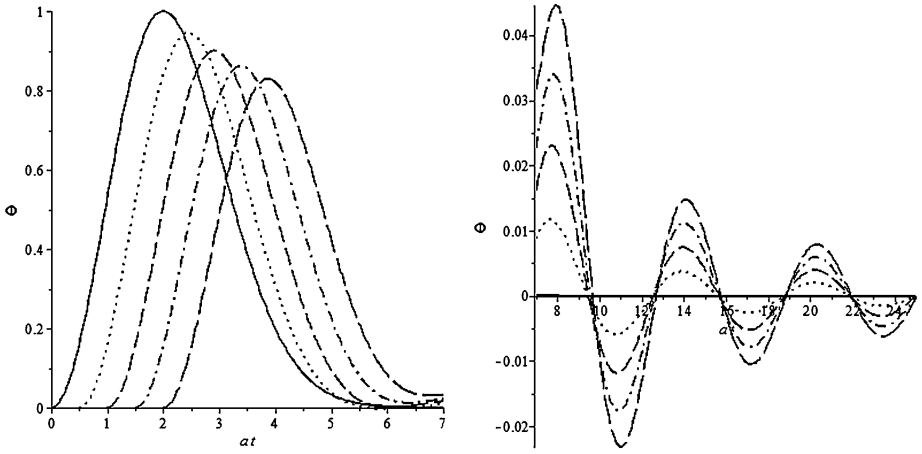

Figure 4 Dependence of the function Φ defined by Equation (33) on $\tilde{t} = at$ at fixed $\tilde{\tau} = a\tau$ for $\zeta = 2$. The solid, dotted, dashed, dashed–dotted, and long-dashed curves correspond to $\tilde{\tau} = 0$, 0.5, 1, 1.5, and 2. The left panel shows the dependence of Φ on $\tilde{t}$ for $\tilde{t} \le 7$, while the right panel shows this dependence for $\tilde{t} \le 25$. There is no solid curve in the right panel because $\Phi \approx 0$ at $\tilde{\tau} = 0$ for $\tilde{t} > 7$.

increases from the loop foot-point to the loop apex and has to be symmetric with respect to the apex, $c_{\rm k}(z)$ is defined by Equation (10) with the parameters satisfying Equation (13). It is convenient to transform Equation (10) to

$$c_{\rm k} = c_{\rm ka} - \frac{a^2}{c_{\rm ka}}(z-\ell)^2, \tag{35}$$

where $c_{\rm ka} = c_{\rm k}(\ell)$ is the kink speed at the loop apex. We recall that ℓ is the loop half-length. It is convenient to introduce the parameter $\kappa = H_{\rm a}/H$, where $H_{\rm a}$ is the loop height and H is the atmospheric scale height. In an isothermal atmosphere, the plasma density is proportional to $\mathrm{e}^{-h/H}$, where h is the height in the atmosphere and $c_{\rm k}$ is inversely proportional to the square root of the density, we therefore obtain $c_{\rm ka}/c_{\rm kf} = \mathrm{e}^{\kappa/2}$, where $c_{\rm kf} = c_{\rm k}(0)$ is the kink speed at the loop foot-point. Using this result and Equation (35) yields

$$a^2 = \frac{2c_{\rm kf}^2}{\ell^2}\left(\mathrm{e}^{\kappa} - \mathrm{e}^{\kappa/2}\right). \tag{36}$$

When κ increases from 0.5 to 2, the cut-off frequency a monotonically increases from $0.6c_{\rm kf}/\ell$ to $2.16c_{\rm kf}/\ell$, while the corresponding period $P_{\rm cut} = 2\pi/a$ monotonically decreases from $10.5\ell/c_{\rm kf}$ to $2.9\ell/c_{\rm kf}$. The fundamental-mode period in a homogeneous loop with the kink speed equal to $c_{\rm kf}$ is $2\ell/c_{\rm kf}$. In a stratified loop $c_{\rm k}(z) > c_{\rm kf}$ for $z > 0$, which means that the fundamental-mode period is shorter than $2\ell/c_{\rm kf}$. We see that for $0.5 \le \kappa \le 2$ the cut-off period is longer than the fundamental-mode period.

Consider now the loop of a half-circle shape. For such a loop $\ell = \pi\kappa H/2$, and we can rewrite Equation (36) as

$$P_{\rm cut} = \frac{\pi^2 \kappa H}{c_{\rm kf}\sqrt{\mathrm{e}^{\kappa} - \mathrm{e}^{\kappa/2}}}. \tag{37}$$

We take $c_{\mathrm{kf}} = 1000\ \mathrm{km\,s^{-1}}$ and $H = 60$ Mm as typical values for coronal loops. Then the loop length varies from 94 Mm to 376 Mm when κ varies from 0.5 to 2. The values of function $\kappa/\sqrt{\mathrm{e}^{\kappa} - \mathrm{e}^{\kappa/2}}$ are between 0.8 and 1 when $\kappa \in [0.5, 2]$, so to obtain estimates for P_{cut} we can take $\kappa/\sqrt{\mathrm{e}^{\kappa} - \mathrm{e}^{\kappa/2}} \approx 0.9$. Then it follows from Equation (37) that $P_{\mathrm{cut}} \approx 0.9\pi^2 H/c_{\mathrm{kf}}$ 530 seconds.

Recently, Nisticò, Nakariakov, and Verwichte (2013) and Anfinogentov, Nisticò, and Nakariakov (2013) reported observations of low-amplitude decay-less kink oscillations in coronal loops. At present, the continual buffeting of the loop foot-points by the sub-photospheric convection is considered as the most probable mechanism of excitation of these oscillations. Some of the observed oscillations have quite long periods, above 500 seconds. Taking this into account, we suggest an alternative mechanism of excitation of the decay-less kink oscillations. If we assume that pulses of kink waves are permanently launched at loop foot-points, then the observed low-amplitude kink oscillations can be oscillations with frequencies close to the cut-off frequency that exist after the leading pulse has passed.

7. Summary and Conclusions

We have studied the propagation of pulses of kink waves on magnetic-flux tubes. We used the thin-tube approximation and assumed that the phase speed of kink waves is either a linear or a quadratic function of the distance along the tube. We briefly described the method of reduction of the wave equation describing the kink wave propagation to the Klein–Gordon equation with constant coefficients.

The pulse propagation of kink waves is described by the initial value–boundary value problem for the Klein–Gordon equation. We assumed that the tube is at rest at the initial moment of time. The wave pulse is launched by the perturbation of the tube footpoint. We presented the general solution for this problem. Using this general solution, we studied the propagation of very short pulses analytically and longer pulses numerically. The signatures of pulse propagation are qualitatively different when there is a cut-off frequency and when it is absent. When there is a cut-off frequency, oscillations with the cut-off frequency emerge after the passage of a short pulse. Their amplitudes decay as $t^{-3/2}$. When the cut-off frequency is absent, a perturbation with a smaller amplitude emerges after the passage of a short pulse. The amplitude of this perturbation grows with time.

We applied the general theory to the propagation of kink pulses in coronal loops. We assumed that the phase speed is a quadratic function of the distance along the loop that has its maximum at the loop apex. We also assumed that the loop has the shape of a half-circle, a circular cross-section of constant radius, and that it is situated in the vertical plane. There is a cut-off frequency for this equilibrium. We derived the general expressions for the cut-off frequency and period. Then we estimated that the cut-off period is about 500 seconds for typical parameters of coronal magnetic loops. We suggested that the oscillations with the cut-off frequency emerging after the passage of the initial short pulse can be one possible mechanisms of the excitation of low-amplitude decay-less kink oscillations recently observed in coronal loops.

Acknowledgements The authors acknowledge the support by the Russian Fund for Fundamental Research (RFBR) grant (13-02-00656). The work of E. Pelinovsky is supported by the Ministry of Education and Science of the Russian Federation (the base part of the state task No. 2014/133 (project 2839)).

Disclosure of Potential Conflicts of Interests The authors declare that they have no conflicts of interests.

Appendix: Solution of Equation (8) with $\beta = -a^2 < 0$

In this section we solve Equation (8) with the initial conditions given by Equation (23) and the boundary condition given by Equation (22). We introduce a function Ψ defined as $\Psi = \Phi - \Phi_0(t)\mathrm{e}^{-a\tau}$. Then Equation (8) reduces to

$$\frac{\partial^2\Psi}{\partial t^2} - \frac{\partial^2\Psi}{\partial\tau^2} = -\Phi_0''(t)\mathrm{e}^{-a\tau}, \tag{38}$$

and the function Ψ satisfies the boundary conditions

$$\Psi(0,t) = 0, \qquad \Psi(\tau,t) \to 0 \quad \text{as } \tau \to \infty, \tag{39}$$

and the initial conditions

$$\Psi(\tau,0) = 0, \qquad \frac{\partial\Psi}{\partial t}(\tau,0) = 0, \tag{40}$$

where we have taken into account that $\Psi_0(0) = \Psi_0'(0) = 0$. Now we introduce the Fourier sine transform with respect to τ,

$$\widehat{\Psi}(\sigma,t) = \int_0^\infty \Psi(\tau,t)\sin(\sigma\tau)\,\mathrm{d}\tau, \qquad \Psi(\tau,t) = \frac{2}{\pi}\int_0^\infty \widehat{\Psi}(\sigma,t)\sin(\sigma\tau)\,\mathrm{d}\sigma. \tag{41}$$

Applying this transform to Equation (38), we obtain

$$\frac{\partial^2\widehat{\Psi}}{\partial t^2} + \left(a^2+\sigma^2\right)\widehat{\Psi} = -\frac{\sigma\Phi_0''(t)}{a^2+\sigma^2}. \tag{42}$$

From Equation (40) we obtain the initial conditions

$$\widehat{\Psi}(\sigma,0) = 0, \qquad \frac{\partial\widehat{\Psi}}{\partial t}(\sigma,0) = 0. \tag{43}$$

To obtain the solution to Equation (42) with the initial conditions (43), we use the method of varying arbitrary constants. The calculation is straightforward, so we give only the final result:

$$\widehat{\Psi}(\sigma,t) = -\frac{\sigma\Phi_0(t)}{a^2+\sigma^2} + \int_0^t \frac{\sigma\Phi_0(\xi)\sin((t-\xi)\sqrt{a^2+\sigma^2})}{\sqrt{a^2+\sigma^2}}\,\mathrm{d}\xi. \tag{44}$$

The function $\Psi(\tau,t)$ is given by the inverse Fourier transform. To calculate it we use the formula (Erdélyi, 1954)

$$\int_0^\infty \frac{\sin(t\sqrt{a^2+\sigma^2})\cos(\sigma\tau)}{\sqrt{a^2+\sigma^2}}\,\mathrm{d}\sigma = \begin{cases} \frac{1}{2}\pi J_0(a\sqrt{t^2-\tau^2}), & 0<\tau<t, \\ 0, & \tau>t, \end{cases} \tag{45}$$

Differentiating this equation with respect to τ, we obtain

$$\int_0^\infty \frac{\sigma\sin(t\sqrt{a^2+\sigma^2})\sin(\sigma\tau)}{\sqrt{a^2+\sigma^2}}\,\mathrm{d}\sigma = \frac{\pi}{2}\delta(\tau-t) - \begin{cases} \frac{\pi a\tau J_1(a\sqrt{t^2-\tau^2})}{2\sqrt{t^2-\tau^2}}, & 0<\tau<t, \\ 0, & \tau>t, \end{cases} \tag{46}$$

where δ is the delta-function. Using this result yields

$$\Psi(\tau,t) = -\Phi_0(t)\mathrm{e}^{-a\tau} + \begin{cases} \Phi(\tau-t) - a\tau\int_0^{t-\tau} \frac{J_1(a\sqrt{(t-\xi)^2-\tau^2})}{\sqrt{(t-\xi)^2-\tau^2}}\,\mathrm{d}\xi, & 0<\tau<t, \\ 0, & \tau>t. \end{cases} \tag{47}$$

Recalling the relation between Ψ and Φ, we arrive at Equation (25).

References

Abramowitz, M., Stegun, I.A.: 1964, *Handbook of Mathematical Functions*, National Bureau of Standards, Washington

Anfinogentov, S., Nisticò, G., Nakariakov, V.M.: 2013, *Astron. Astrophys.* **560**, A107. DOI.

Budak, B.M., Samarski, A.A., Tikhonov, A.N.: 1964, *A Collection of Problems on Mathematical Physics*, Pergamon, Oxford.

Cally, P.S.: 2012, *Solar Phys.* **280**, 33. DOI.

Erdélyi, A.: 1954, *Table of Integrals Transforms, vol. 1*, McGraw-Hill, New York.

Kuridze, D., Morton, R.J., Erdélyi, R., Dorrian, G.D., Mathioudakis, M., Jess, D.B., Keenan, F.P.: 2012, *Astrophys. J.* **750**, 51. DOI.

Lin, Y., Engvold, O., Rouppe van der Voort, L.H.M., van Noort, M.: 2007, *Solar Phys.* **246**, 65. DOI.

Nisticò, G., Nakariakov, V.M., Verwichte, E.: 2013, *Astron. Astrophys.* **552**, A57. DOI.

Okamoto, T.J., Tsuneta, S., Berger, T.E., Ichimoto, K., Katsukawa, Y., Lites, B.W., *et al.*: 2007, *Science* **318**, 1577. DOI.

Oliver, R., Ruderman, M.S., Terradas, J.: 2014, *Astrophys. J.* **789**, A48. DOI.

Petrukhin, N.S., Pelinovsky, E.N., Batsyna, E.K.: 2012, *Astron. Lett.* **38**, 388. DOI.

Pietarila, A., Aznar Cuadrado, R., Hirzberger, J., Solanki, S.K.: 2011, *Astrophys. J.* **739**, 92. DOI.

Rae, I.C., Roberts, B.: 1982, *Astrophys. J.* **256**, 761. DOI.

Ruderman, M.S., Verth, G., Erdélyi, R.: 2008, *Astrophys. J.* **686**, 694. DOI.

Ruderman, M.S., Pelinovsky, E., Petrukhin, N.S., Talipova, T.: 2013, *Solar Phys.* **286**, 417. DOI.

Terradas, J., Goossens, M., Verth, G.: 2010, *Astron. Astrophys.* **524**, A23. DOI.

Tian, H., McIntosh, S.W., Wang, T., Ofman, L., De Pontieu, B., Innes, D.E., Peter, H.: 2012, *Astrophys. J.* **759**, 144. DOI.

Tomczyk, S., McIntosh, S.W.: 2009, *Astrophys. J.* **697**, 1384. DOI.

Tomczyk, S., McIntosh, S.W., Keil, S.L., Judge, P.G., Schad, T., Seeley, D.H., Edmondson, J.: 2007, *Science* **317**, 1192. DOI.

Verth, G., Terradas, J., Goossens, M.: 2010, *Astrophys. J. Lett.* **718**, L102. DOI.

Zaqarashvili, T.V., Khutsishvili, E., Kukhianidze, V., Ramishvili, G.: 2007, *Astron. Astrophys.* **474**, 627. DOI.

Zeldovich, I.B., Novikov, I.D.: 1975, *Structure and Evolution of the Universe*, Nauka, Moscow (in Russian).